Multi-beam Modulated Metasurface Antenna for Backhaul Applications at K-band

Jorge Ruiz-García[1], *Marco Faenzi*[1], *Adham Mahmoud*[1], *Mauro Ettorre*[1], *Patrick Potier*[2], *Philippe Pouliguen*[3], *Ronan Sauleau*[1], *and David González-Ovejero*[1]

[1] *Univ. Rennes, CNRS, IETR - UMR 6164, F-35000, Rennes, France, jorge.ruiz@univ-rennes1.fr*
[2] *Direction Générale de l'Armement, 35174 Bruz, France*
[3] *Direction Générale de l'Armement, Agence de l'innovation de défense, 75509 Paris, France*

Abstract:

We explore the use of a new modulated metasurface (MTS) antenna topology as solution for wireless backhaul at K band. The proposed structure is composed of a quasi-optical beamformer, which feeds the modulated MTS radiating aperture. These two elements are vertically stacked in a two-layer pillbox architecture to produce a very compact antenna. Furthermore, our design is able to provide several beams at different pointing angles and, hence, it offers the possibility of discrete beam steering by beam switching. The employment of a modulated MTS and the compactness given by the pillbox approach lead to a high-gain and low-profile antenna that could be an appealing solution for mobile backhaul networks.

1   Introduction

Microwaves and millimeter waves frequencies are among the frequency bands allocated for small-cell backhaul in 5G networks [1]. The use of metasurfaces (MTSs) for 5G systems has been studied and proved to be extremely useful in the aforementioned frequency ranges. Indeed, some antenna prototypes based on MTSs have already been developed with the aim of satisfying the needs of the new generation of mobile networks [2, 3]. Modulated MTS antennas, which were initially developed for satellite communications, are a special category of MTS antennas [4]. The low profile, low cost and reduced power consumption of this kind of structures, along with the adaptability of the design process to different frequencies, make them a very attractive solution.

A MTS is generally formed by sub-wavelength elements arranged on a periodic lattice and either printed on a grounded dielectric slab or grown on a metallic base-plate. By changing the geometry of these constitutive elements in the lattice unit-cell, one can exert a high degree of control on the aperture fields [5, 6, 7]. The MTS layer can be modeled as a continuous impedance boundary condition (IBC) due to the small size of the elements compared to the wavelength. In modulated MTS antennas, a surface wave (SW) is excited on the aperture and gradually transformed into a leaky-wave owing to its interaction with the periodically modulated IBC, which results in a radiated beam [8]. By tuning the properties of the modulation one can control the attributes of the beam, such as the pointing angle, shape, and polarization.

This paper presents a modulated MTS antenna operating at K-band with multibeam performance. The system is based on a pillbox quasi-optical beamformer [9], which essentially transforms the cylindrical wave propagating on the pillbox's lower layer into a plane wave in the upper layer. By adding a modulated MTS on the top layer (Figure 1a), one obtains a compact antenna. A pillbox-fed modulated MTS antenna at X-band was described in [10]. As mentioned before, the entire design process can be adapted for other frequency bands by properly modifying the material, the beamformer, and the MTS elements dimensions. Thus, in this work, we use a strategy similar to that described in [10] to design an antenna operating at $f_o = 20.7$ GHz.

2   Design of a Multi-beam Modulated Metasurface Antenna

In the following, we will refer to the Cartesian reference system (x,y,z) shown in Figure 1a. The IBC used to model our MTS consists in a sheet transition [11, 12], penetrable [13] or transparent impedance [14, 15] $Z_s = jX_s$ which lies on top of a grounded dielectric slab. This structure supports the propagation of a TM surface wave. In order to get the desired radiation effect, the sheet transition impedance is modulated along x-direction as

$$X_s(x) = X_{av}(1 + M(x)\cos(2\pi x/p)), \tag{1}$$

where X_{av} is the average reactance, $M(x)$ is the modulation index ($0 \leq M(x) \leq 1$) and p is the period. The chosen material is Rogers RO3006 ($\varepsilon_r = 6.15$, $\tan\delta = 0.002$) with thickness $h = 0.64$mm. In order to implement

(a) Side view of total structure

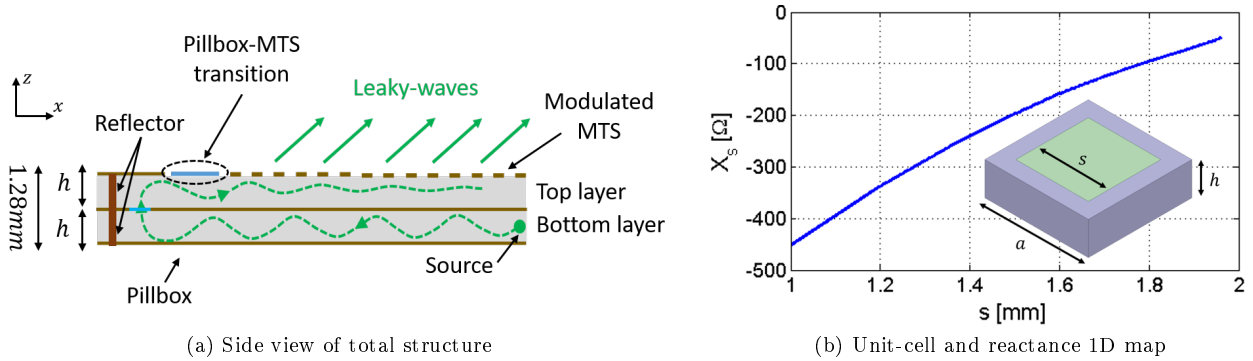(b) Unit-cell and reactance 1D map

Figure 1 – (a) Side view of the pillbox fed MTS antenna. (b) Unit-cell with square metallic patch and curve representing $X_s(s)$ for different patch sizes.

(1), we use square metallic patches whose size changes according to the spatial variation of $X_s(x)$. To that end, we first build a database that relates the patch dimensions to the sheet transition IBC values. Taking a unit-cell (a single MTS element) of side a on a substrate of thickness h, and assuming it inside a regular lattice to preserve the local periodicity principle, one can vary progressively the metallic patch size s and extract the equivalent sheet impedance Z_s. Figure 1b shows the curve that relates both parameters as well as an inset with the geometry of the unit-cell. The MTS element has a constant size $a = \lambda_0/7$, which makes it small compared to the SW wavelength, as indicated in Section 1. Once we have characterized the unit-cell, the next design step consists in retrieving the square patch dimensions that better match the ideal values in (1) to obtain our modulated MTS. The latter is placed then on the beamfomer top layer to get the final structure depicted in Figure 2a.

In addition, it is important to note that the use of a pillbox allows one to place several sources (here, H-plane horns) in the bottom layer. These horns are arranged at the focal plane of the pillbox's reflector (Figure 2a) and each one provides a beam pointing at a different direction. Indeed, when the source position is shifted in the focal plane (along y-direction), the direction of propagation of the resulting plane-wave changes. As a result, the placement of N ports originates up to N beams at different pointing angles. This feature will be illustrated in the next section. Obviously, the number of sources is limited by the pillbox dimension, the horn size, and the HPBW of the radiated beams. The antenna dimensions are sketched in Figure 1a and Figure 2a, from where we emphasize a very low profile, with a total thickness of 1.28 mm.

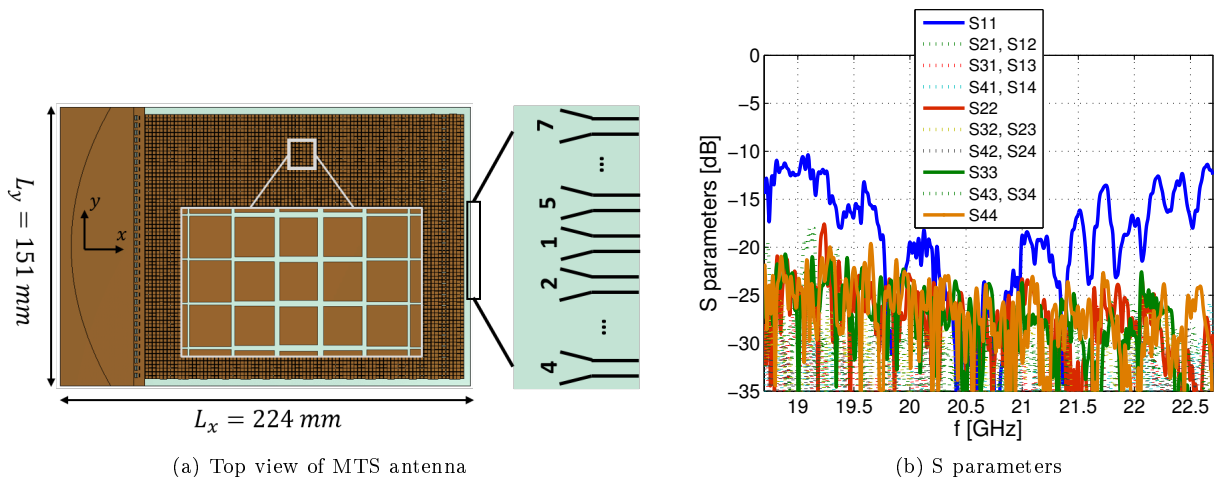(a) Top view of MTS antenna

(b) S parameters

Figure 2 – (a) Disposition of patches and ports in the pillbox beamformer. (b) S-parameters for central and side ports, remaining ports behave as their symmetric ones.

3 Simulation Results

For the design at hand, we implement (1) to obtain a beam at $\theta_0 = 15^o$ for normal incidence (port 1, $\phi_0 = 0^o$). The employed modulation parameters are $p = 11.3$ mm, $X_{av} = -0.24\eta_0$ (where η_0 is the free-space impedance), and M varying with x to optimize the attenuation of the aperture fields and, therefore, enhance the aperture

efficiency of the antenna [16]. Switching between the $N = 7$ ports implies the modification of both θ_0 and ϕ_0. The simulated S-parameters of the horns are shown in Figure 2b, showing a bandwidth of 20% and a very good isolation between ports. Figure 3 presents the radiated beams for each source at f_o. The obtained angular coverage is displayed in Figure 3a, where the direction of the beam is given in (θ, ϕ) coordinates. Next, we represent in Figure 3b the radiation pattern in elevation at the E-plane for every port. The patterns are plotted by cutting every 3D beam at the angle $\phi = \phi_0$, where ϕ_0 is the azimuth angle of maximum gain for each source. The maximum realized gain at f_o is $G = 27.1$ dB for port 1 and the beam-switching losses are up to 2.5dB (realized gain difference between port 1 and ports 4, 7). We note that the generated beams own the property of frequency scanning in θ. Thus, it would be possible to operate at other frequencies around f_o within the bandwidth shown in Figure 2b, modifying then the individual beam directions and the angular coverage.
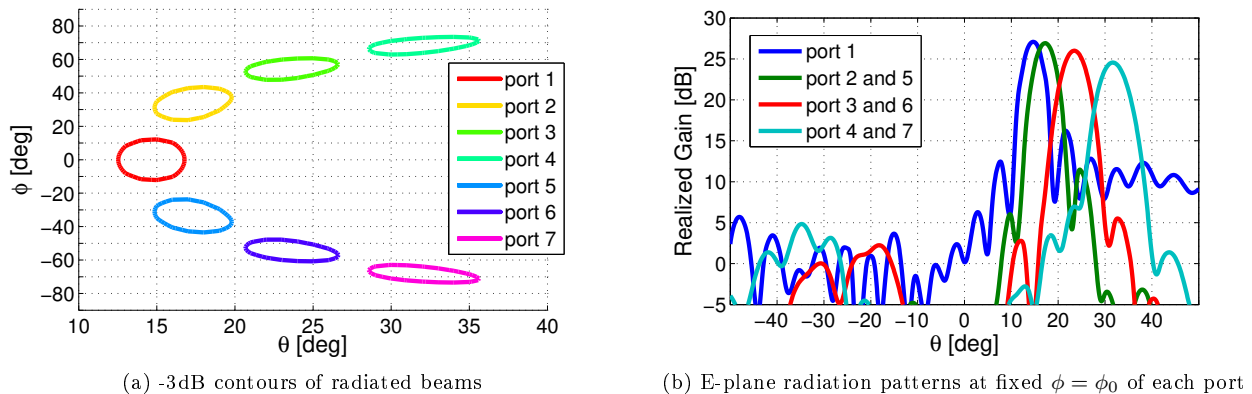

(a) -3dB contours of radiated beams

(b) E-plane radiation patterns at fixed $\phi = \phi_0$ of each port

Figure 3 − (a) Radiation performance in (θ, ϕ) plane, and (b) realized gain at the E-plane cut for each horn.

4 Conclusion

We presented the design and numerical results of a compact modulated MTS antenna at 20.7 GHz. The radiating aperture consists of metallic patches whose size is modified to produce an equivalent modulated impedance. The MTS antenna is fed by a plane SW, which is obtained by means of a quasi-optical beamformer in a pillbox architecture. Moreover, one can change the propagation direction of this SW by exciting different ports in the pillbox focal plane. The proposed antenna topology is able to generate high-gain beams at different pointing angles, while providing a good scanning range in θ and a wide angular coverage in ϕ. The extremely thin profile of the structure ($h_{total} = 1.28mm$), the high-gain behavior, and the multi-beam capability make this antenna a suitable candidate for backhaul applications. Last but not least, this flat aperture antenna can be easily integrated with a low visual impact on smart urban furniture, buildings, homes, and offices.

5 Acknowledgments

6 References

[1] M. M. Ahamed and S. Faruque, "5G backhaul: Requirements, challenges, and emerging technologies," in *Broadband Communications Networks* (A. Haidine and A. Aqqal, eds.), ch. 4, Rijeka: IntechOpen, 2018.

[2] S. Gupta, Z. Briqech, A. R. Sebak, and T. Ahmed Denidni, "Mutual-coupling reduction using metasurface corrugations for 28 GHz MIMO applications," *IEEE Antennas Wireless Propag. Lett.*, vol. 16, pp. 2763–2766, 2017.

[3] T. Li and Z. N. Chen, "Metasurface-based shared-aperture 5G S-/K-band antenna using characteristic mode analysis," *IEEE Trans. Antennas Propag.*, vol. 66, pp. 6742–6750, Dec 2018.

[4] M. Faenzi *et al.*, "Metasurface antennas: New models, applications and realizations," *Sci. Rep.*, vol. 9, p. 10178, July 2019.

[5] S. Maci, G. Minatti, M. Casaletti, and M. Bosiljevac, "Metasurfing: Addressing waves on impenetrable metasurfaces," *IEEE Antennas Wireless Propag. Lett.*, vol. 10, pp. 1499–1502, 2011.

[6] D. González-Ovejero, G. Minatti, G. Chattopadhyay, and S. Maci, "Multibeam by metasurface antennas," *IEEE Trans. Antennas Propag.*, vol. 65, pp. 2923–2930, Jun. 2017.

[7] D. González-Ovejero, N. Chahat, R. Sauleau, G. Chattopadhyay, S. Maci, and M. Ettorre, "Additive manufactured metal-only modulated metasurface antennas," *IEEE Trans. Antennas Propag.*, vol. 66, pp. 6106–6114, Nov 2018.

[8] A. Oliner and A. Hessel, "Guided waves on sinusoidally-modulated reactance surfaces," *IRE Trans. Antennas Propag.*, vol. 7, pp. 201–208, Dec. 1959.

[9] M. Ettorre, R. Sauleau, and L. Le Coq, "Multi-beam multi-layer leaky-wave SIW pillbox antenna for millimeter-wave applications," *IEEE Trans. Antennas Propag.*, vol. 59, pp. 1093–1100, April 2011.

[10] J. Ruiz-García, D. González-Ovejero, M. Faenzi, A. Mahmoud, M. Ettorre, P. Potier, P. Pouliguen, and R. Sauleau, "Quasi-optical excitation of modulated metasurface antennas," in *13th Int. Congress on Artificial Materials for Novel Wave Phenomena (Metamaterials)*, pp. X–348–X–350, Sep. 2019.

[11] E. F. Kuester, M. Mohamed, M. Piket-May, and C. Holloway, "Averaged transition conditions for electromagnetic fields at a metafilm," *IEEE Trans. Antennas Propag.*, vol. 51, pp. 2641–2651, Oct. 2003.

[12] A. M. Patel and A. Grbic, "Effective surface impedance of a printed-circuit tensor impedance surface (PCTIS)," *IEEE Trans. Microw. Theory Tech.*, vol. 61, pp. 1403–1413, April 2013.

[13] E. Bleszynski, M. Bleszynski, and T. Jaroszewicz, "Surface-integral equations for electromagnetic scattering from impenetrable and penetrable sheets," *IEEE Antennas Propag. Mag.*, vol. 35, pp. 14–25, Dec. 1993.

[14] D. González-Ovejero and S. Maci, "Gaussian ring basis functions for the analysis of modulated metasurface antennas," *IEEE Trans. Antennas Propag.*, vol. 63, pp. 3982–3993, Sep. 2015.

[15] G. Minatti, F. Caminita, E. Martini, M. Sabbadini, and S. Maci, "Synthesis of modulated-metasurface antennas with amplitude, phase, and polarization control," *IEEE Trans. Antennas Propag.*, vol. 64, pp. 3907–3919, Sept 2016.

[16] D. R. Jackson and A. A. Oliner, "Leaky–wave antennas," in *Modern antenna handbook* (C. A. Balanis, ed.), ch. 7, pp. 325–367, Wiley, 2007.